

# MECHANICAL STRESS STATES IN HETEROGENEOUS, WOUND ROLLS<sup>1</sup>

SAND--90-3049C

DE91 009257

Robert C. Reuter, Jr.  
 Sandia National Laboratories  
 Albuquerque, New Mexico 87185

## ABSTRACT

This paper presents a method of predicting the internal stress states in rolls wound with simultaneous supply spools of dissimilar material. The method is based on linear, orthotropic behavior of the mandrel and web materials, and is sufficiently general to allow completely arbitrary choices for the web materials and their respective winding tensions. The generality of the method also permits the introduction and termination of additional webs of arbitrary material at any time during the winding process. The method is analytical, and utilizes an elasticity solution with rigorous satisfaction of boundary conditions between each ply of the wound roll. A prototypical wound capacitor is used as an example to provide for numerical results of the internal stress states induced during the winding process. Differences in the winding tension loss of the two dissimilar web materials is discussed and explained, as are other mechanical threats to roll stability and performance. The influence of winding tension variations on internal, wound stress states is also discussed.

## NOMENCLATURE

<u>SYMBOL</u>	<u>DESIGNATES</u>	<u>SUBSCRIPT</u>	<u>DESIGNATES</u>
E	Elastic modulus	M	Mandrel
N	Total number of plies	j,n	Ply indices
P	Pressure acting on ply	n	Stage of winding
r	Variable radius	jn	jth ply at nth stage
R	Specific radius	r,θ	Polar Coordinates
t	Ply thickness		
u	Radial displacement		
ε	Strain		
ν	Poisson's ratio		
σ	Stress		

MASTER

<sup>1</sup>This work performed at Sandia National Laboratories supported by the U.S. Department of Energy under contract number DE-AC04-76DP00789.

## **DISCLAIMER**

**This report was prepared as an account of work sponsored by an agency of the United States Government. Neither the United States Government nor any agency thereof, nor any of their employees, makes any warranty, express or implied, or assumes any legal liability or responsibility for the accuracy, completeness, or usefulness of any information, apparatus, product, or process disclosed, or represents that its use would not infringe privately owned rights. Reference herein to any specific commercial product, process, or service by trade name, trademark, manufacturer, or otherwise does not necessarily constitute or imply its endorsement, recommendation, or favoring by the United States Government or any agency thereof. The views and opinions of authors expressed herein do not necessarily state or reflect those of the United States Government or any agency thereof.**

---

## **DISCLAIMER**

**Portions of this document may be illegible in electronic image products. Images are produced from the best available original document.**

## INTRODUCTION

Several products are fabricated by simultaneously winding webs of dissimilar materials from multiple supply rolls over a rotating mandrel. A cylindrical, high energy density capacitor, with independent conducting paths separated by dielectric material, is an example. A ply pattern of one dielectric, one conductor, three dielectric, one conductor, and two dielectric wound with each turn of the mandrel, from independent supply rolls, produces an eight ply capacitor. Since the webs are wound under tension, mechanical stresses will be induced in the wound portion of the capacitor roll during fabrication. These stresses may produce undesirable processing effects, such as ply buckling, ply slipping and dielectric thinning which could impact product reliability. Therefore, an understanding of the mechanical stress states in these heterogeneous capacitor rolls, which are a direct consequence of the winding process, is highly desirable. There is ample literature documenting the winding analysis of homogeneous rolls, (1-3) to mention only a few, but little with regard to heterogeneous roll construction (4-6).

Two methods have been developed for the analysis of heterogeneous roll construction. The first, called the equivalent layer method (5,7), treats all plies wound during one mandrel revolution as a single, equivalent, orthotropic layer. The second method, which is the subject of this paper, is called the individual ply method. This method retains the identity of each individual ply, and was developed to permit interrupted winding patterns or the introduction of interstitial layers such as miniature cooling ducts. The individual ply method is computationally more time consuming than the equivalent layer method, however, the difference is significant only when large problems are solved.

While the present theory has sufficient generality to permit any material of any thickness under any winding tension in any ply of the roll, the capacitor with its repetitive ply pattern serves as a realistic example of heterogeneous, wound construction. Numerical examples of a generic, eight ply capacitor wound with simple winding tension profiles are presented, and consequences of heterogeneous construction are discussed.

## ANALYTICAL DEVELOPMENT

The problem is cast in the framework of linear elasticity with orthotropic material behavior, circular, cylindrical roll construction, and plane stress in the roll cross section. The assumption of polar symmetry permits all plies to be represented as concentric cylinders which are accreted sequentially, the outer most ply at any stage of winding being applied with its winding tension. All buried plies experience winding tension loss according to their relative position in the roll and the mechanical and physical properties of the roll constituents. The mandrel over which the plies are wound is also elastic and orthotropic.

Constitutive behavior, strain-displacement relations, and radial equilibrium respectively, are given by the following.

$$\sigma_r = \frac{E_r}{(1 - \nu_{r\theta}\nu_{\theta r})}(\epsilon_r + \nu_{r\theta}\epsilon_\theta) \quad (1)$$

$$\sigma_\theta = \frac{E_\theta}{(1 - \nu_{r\theta}\nu_{\theta r})}(\nu_{\theta r}\epsilon_r + \epsilon_\theta)$$

Received by OSTI

MAR 22 1991

$$\epsilon_r = \frac{du}{dr}, \quad \epsilon_\theta = \frac{u}{r} \quad (2)$$

$$\frac{d\sigma_r}{dr} + \frac{(\sigma_r - \sigma_\theta)}{r} = 0 \quad (3)$$

$$\theta_j = \frac{\mu_j}{(\theta_{j-1}\lambda_{j-1} - \lambda_j + \mu_{j-1})} \quad , \quad \phi_j = \frac{-\phi_{j-1}\lambda_{j-1}}{(\theta_{j-1}\lambda_{j-1} - \lambda_j + \mu_{j-1})} \quad (11)$$

The average circumferential stress in any ply is of interest since it can be related directly to the original winding tension and to the wound tension of that ply. It is obtained by integrating the second equation of (7) as follows.

$$\bar{\sigma}_{\theta j} = \frac{1}{(R_{j+1} - R_j)} \int_{R_j}^{R_{j+1}} \sigma_{\theta j} dr \quad (12)$$

Carrying out the integration in (12) yields the result.

$$\bar{\sigma}_{\theta j} = \frac{(P_j R_j - P_{j+1} R_{j+1})}{(R_{j+1} - R_j)} \quad (13)$$

## NUMERICAL SOLUTION

Obtaining a numerical solution for displacements and stresses in the partially wound or completed roll proceeds directly. As stated earlier, the outermost ply at any stage of winding,  $n$ , retains its winding tension, or winding stress,  $\bar{\sigma}_{\theta Wn}$ . The internal pressure,  $P_n$ , acting on the  $n$ th ply to equilibrate its winding tension can be calculated directly from (13).

$$P_n = \frac{(R_{n+1} - R_n)}{R_n} \bar{\sigma}_{\theta Wn} \quad (14)$$

Knowing  $P_n$ , all other interface pressures can be calculated successively by using (9). Displacements and stresses are then obtained from (5), (7), and (12). This calculation is performed for all stages of winding (ie., for all values of  $n$  for  $1 \leq n \leq N$ ), and the results are summed. To clarify this process, a pair of subscripts,  $jn$ , is introduced to indicate reference to the  $j$ th ply after the  $n$ th stage of winding. Then, results after any stage of winding can be expressed in the following form.

$$\begin{aligned} u_{jn} &= \sum_{k=1}^n u_{jk} \quad , \quad j \leq k \quad , \quad 1 \leq n \leq N \\ \sigma_{rjn} &= \sum_{k=1}^n \sigma_{rjk} \quad , \quad j \leq k \quad , \quad 1 \leq n \leq N \\ \bar{\sigma}_{\theta jn} &= \sum_{k=1}^n \sigma_{\theta jk} \quad , \quad j \leq k \quad , \quad 1 \leq n \leq N \end{aligned} \quad (15)$$

The mechanical state in the roll at the conclusion of the winding process is obtained from (15) by replacing  $n$  by  $N$ . A computer code was written to facilitate these calculations.

## NUMERICAL EXAMPLE

The eight ply capacitor chosen for the numerical example has aluminum conductor and mylar dielectric webs which are wound over a solid, 7.925mm diameter paper phenolic mandrel. The following material and physical properties apply.

Material	Ply No.	$E_r$ (MPa)	$E_\theta$ (MPa)	$\nu_{r\theta}$	t (in)
Aluminum	2,6	$6.89 \cdot 10^4$	$6.89 \cdot 10^4$	0.33	$5.08 \cdot 10^{-3}$
Mylar	1,3,4,5,7,8	$1.72 \cdot 10^2$	$4.41 \cdot 10^3$	.017	$1.016 \cdot 10^{-2}$
Paper Phenolic	—	$6.89 \cdot 10^3$	$6.89 \cdot 10^3$	0.40	—

The winding pattern consists of 10 blank mylar plies followed by a repeated sequence of one mylar, one aluminum, three mylar, one aluminum, two mylar plies for two hundred sixty three (263) turns of the mandrel, producing a total of 2114 plies in the completed capacitor.

Wound tensions and radial stresses for this capacitor construction, as wound with 2.4 Newtons constant winding tension in all plies, tension Case 1, are shown in Figs 1 and 2, respectively. As seen in Fig 1, there is some wound tension variation throughout the capacitor in the mylar plies, however, these values do not differ significantly from the original winding tension of 2.4 Newtons, and they are always tensile. The wound tensions in the aluminum plies are compressive throughout most of the capacitor, having lost more tension than that with which they were originally wound. The aluminum plies in only the outer 7% of the capacitor remain tensile, and with only the outer most ply (mylar) retaining its original winding tension, which is consistent with an earlier assumption.

An explanation for the large difference in tension loss between the aluminum and mylar plies is straightforward. Imbedded, adjacent plies of mylar and aluminum experience nearly the same change in strain, moving radially inward, as subsequent plies are wound. Comparable strains in the two materials produce significantly greater tension losses in the aluminum, because it is significantly stiffer than mylar (see the Table above). Another interesting feature of the curves in Fig 1 is the tension variation in a region near the mandrel. Both materials experience their steepest wound tension gradients in this region, where the potential for circumferential slipping is greatest. This is a direct consequence of the stiffness of the mandrel chosen for this example, which is comparatively high. The mandrel does not permit as much relaxation (and therefore, tension loss) of adjacent and nearby plies as does a foundation of wound plies at larger radii. As the radial dimension of the ply foundation grows, its stiffness diminishes to a value consistent with that of only the wound capacitor plies, i.e., where the mandrel has lost its stiffening influence. A softer mandrel would flatten the curves in its vicinity, or could even reverse the sign of the tension gradients. The control of circumferential slippage in a wound roll may influence mandrel design and material choices.

Radial stress (internal pressure), Fig 2, shows its highest value at the mandrel, again a consequence of a relatively stiff mandrel. The sudden decline in radial stress magnitude is caused by the sudden decline in wound tension, Fig 1. A softer mandrel would flatten or reverse this radial stress variation near the mandrel. The radial stress curve is nearly constant in the nearly constant wound tension regions of the capacitor, and reaches a zero value at the traction free surface of the capacitor. The heavy line thickness of the radial stress curve in Fig 2 is caused by the saw tooth nature of the curve, which can be seen when plotted on an enlarged scale. While tensile values of wound tension in the mylar plies cause a gradual reduction in the radial stress magnitude (the general trend of the curve in Fig 2), the compressive values in the aluminum plies cause an increase in radial stress magnitude, thus the saw tooth shape.

Figures 3 and 4 illustrate the consequences of reducing the winding tension in only the mylar plies from 2.4 Newtons to 1.2 Newtons. Clearly, the wound tension magnitudes are reduced, and the tension loss is somewhat reduced as well. Of greater significance is the effect that mylar ply winding tension reduction has on the wound tension in the aluminum plies. While the wound tension in these plies is still compressive throughout most of the capacitor, the magnitudes have been substantially reduced, thus diminishing the threat of ply instability. Some level of compressive load in the aluminum plies can be tolerated without loss of stability since they are supported laterally between mylar plies under tensile load. The tension loss gradient near the mandrel has also diminished, reducing the threat of circumferential ply slippage. Radial stresses for this winding tension pattern are also reduced, as seen in Fig 4, thus reducing dielectric ply thinning.

Overall, winding the softer mylar plies with lower tensions than the stiffer aluminum plies appears to offer several benefits.

Many other combinations of roll constituent properties and winding tension patterns produce other interesting results, but their presentation is beyond the scope of this paper. It is

These equations produce the single governing Cauchy equation in the radial displacement,  $u$ , as a function of radial position,  $r$ .

$$\frac{d^2u}{dr^2} + \frac{1}{r} \frac{du}{dr} - \alpha^2 \frac{u}{r^2} = 0 \quad , \quad \alpha^2 = \frac{E_\theta}{E_r} \quad (4)$$

Equation (4) has the following general solution which is subscripted for reference to the  $j$ th ply.

$$u_j(r) = \frac{(1 - \nu_{r\theta j} \nu_{\theta r j})}{E_{rj}(R_{j+1}^{2\alpha_j} - R_j^{2\alpha_j})} \left[ (P_j R_j^{\alpha_j+1} - P_{j+1} R_{j+1}^{\alpha_j+1}) \frac{r^{\alpha_j}}{(\alpha_j + \nu_{r\theta j})} \right. \\ \left. - (R_j R_{j+1})^{\alpha_j+1} (P_j R_{j+1}^{\alpha_j-1} - P_{j+1} R_j^{\alpha_j-1}) \frac{r^{-\alpha_j}}{(\alpha_j - \nu_{r\theta j})} \right] \quad (5)$$

In (5),  $P_j$  and  $P_{j+1}$  are the pressures on the inner and outer surfaces, and  $R_j$  and  $R_{j+1}$  are the radii of the inner and outer surfaces of the  $j$ th ply, respectively. Equation (5) can be rewritten for convenience in the following form.

$$u_j(r) = P_j \lambda_j(r) + P_{j+1} \mu_j(r) \quad (6)$$

where

$$\lambda_j(r) = \frac{(1 - \nu_{r\theta j} \nu_{\theta r j}) R_j^{\alpha_j+1}}{E_{rj}(R_{j+1}^{2\alpha_j} - R_j^{2\alpha_j})} \left[ \frac{r^{\alpha_j}}{(\alpha_j + \nu_{r\theta j})} + \frac{R_{j+1}^{2\alpha_j}}{r^{\alpha_j} (\alpha_j - \nu_{r\theta j})} \right] \\ \mu_j(r) = \frac{-(1 - \nu_{r\theta j} \nu_{\theta r j}) R_{j+1}^{\alpha_j+1}}{E_{rj}(R_{j+1}^{2\alpha_j} - R_j^{2\alpha_j})} \left[ \frac{r^{\alpha_j}}{(\alpha_j + \nu_{r\theta j})} + \frac{R_j^{2\alpha_j}}{r^{\alpha_j} (\alpha_j - \nu_{r\theta j})} \right]$$

Corresponding radial and circumferential stresses of the  $j$ th ply follow.

$$\sigma_{rj} = \frac{1}{(R_{j+1}^{2\alpha_j} - R_j^{2\alpha_j})} \left[ (P_j R_j^{\alpha_j+1} - P_{j+1} R_{j+1}^{\alpha_j+1}) r^{\alpha_j-1} + (R_j R_{j+1})^{\alpha_j+1} (P_{j+1} R_j^{\alpha_j-1} - P_j R_{j+1}^{\alpha_j-1}) r^{-\alpha_j-1} \right] \quad (7)$$

$$\sigma_{\theta j} = \frac{\alpha_j}{(R_{j+1}^{2\alpha_j} - R_j^{2\alpha_j})} \left[ (P_j R_j^{\alpha_j+1} - P_{j+1} R_{j+1}^{\alpha_j+1}) r^{\alpha_j-1} - (R_j R_{j+1})^{\alpha_j+1} (P_{j+1} R_j^{\alpha_j-1} - P_j R_{j+1}^{\alpha_j-1}) r^{-\alpha_j-1} \right]$$

Compatibility between all adjacent ply interfaces requires that the following conditions are met.

$$u_j(R_{j+1}) = u_{j+1}(R_{j+1}) \quad , \quad j = M, 1, 2, \dots, n - 1 \quad (8)$$

Substitution of (6) into (8) and solving for the pressures gives a set of algebraic equations from which all interface pressures can be calculated from the  $(n-1)$ th ply to the 1st ply.

$$P_{n-1} = \theta_{n-1} P_n + \phi_{n-1} \\ \vdots \\ P_j = \theta_j P_{j+1} + \phi_j \quad (9) \\ \vdots \\ P_1 = \theta_1 P_2 + \phi_1$$

where

$$\theta_1 = \frac{\mu_1}{(\mu_M - \lambda_1)} \quad , \quad \phi_1 = \frac{-P_M \lambda_M}{(\mu_M - \lambda_1)} \quad (10)$$

### CIRCUMFERENTIAL TENSION IN WOUND CAPACITOR

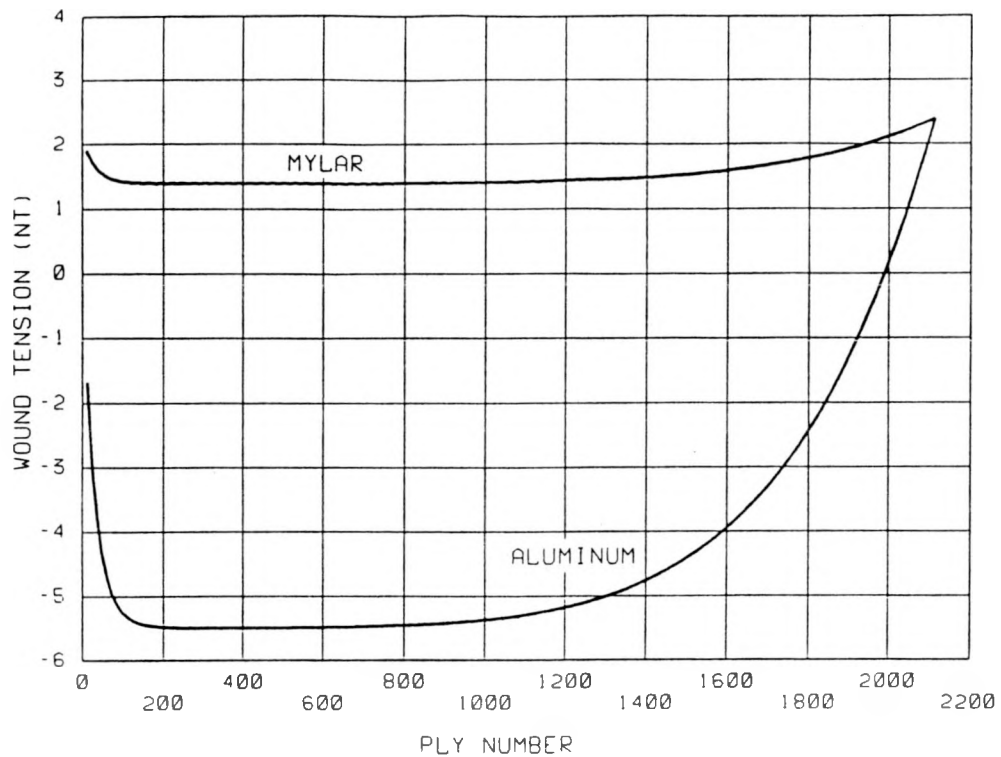


Fig. 1 Circumferential tensions for winding tension Case 1 (2.4 Newtons all plies).

### RADIAL STRESSES IN WOUND CAPACITOR

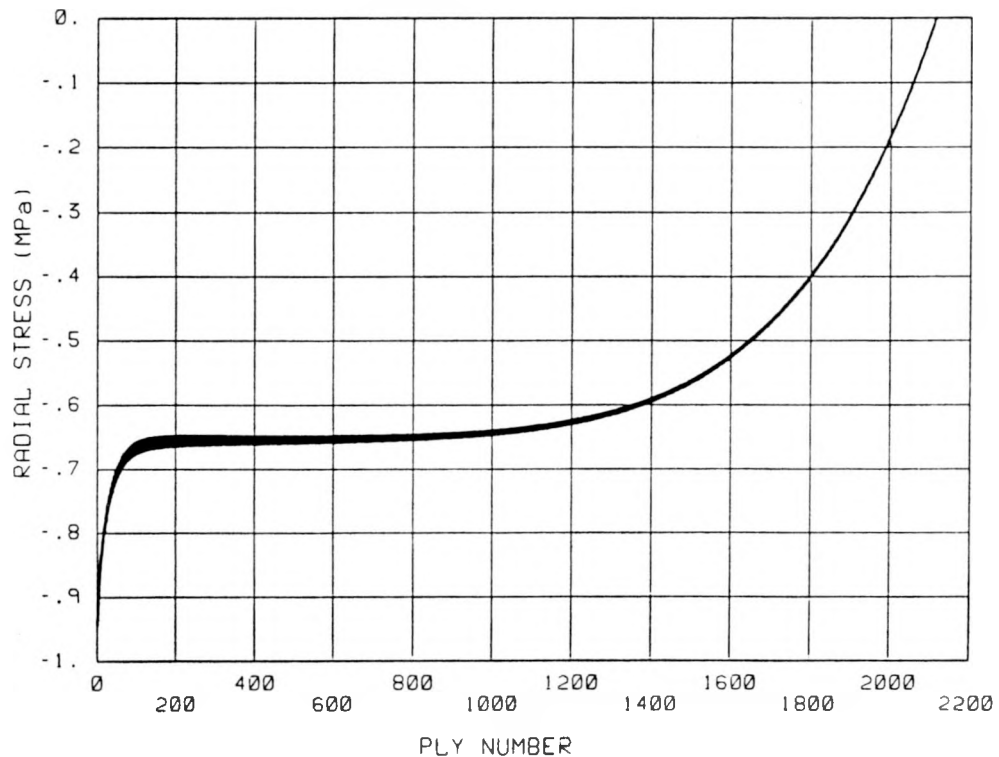


Fig. 2 Radial stresses for winding tension Case 1 (2.4 Newtons all plies).

### CIRCUMFERENTIAL TENSION IN WOUND CAPACITOR

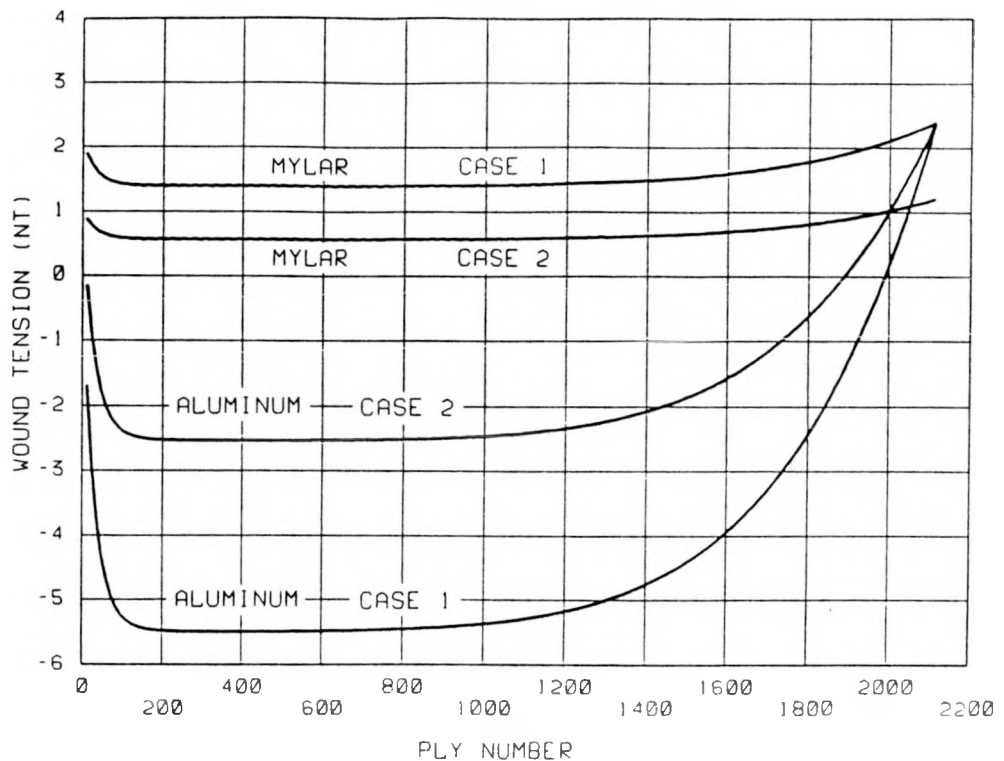


Fig. 3 Circumferential tensions for winding tension Cases 1 and 2 (Case 1 - 2.4 Newtons all plies; Case 2 - 1.2 Newtons mylar plies, 2.4 Newtons aluminum plies).

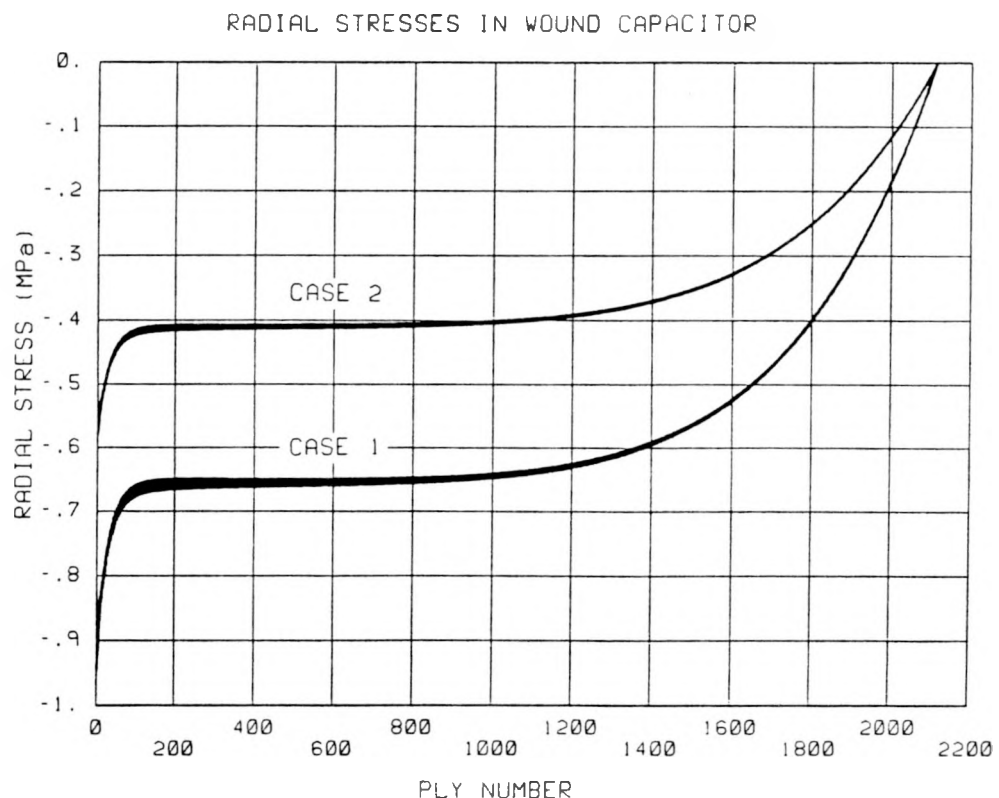


Fig. 4 Radial stresses for winding tension Cases 1 and 2 (Case 1 - 2.4 Newtons all plies; Case 2 - 1.2 Newtons mylar plies, 2.4 Newtons aluminum plies).

evident, however, that heterogeneous construction produces complex mechanical stress states with interesting interdependence.

## CLOSURE

Heterogeneous construction in wound rolls has produced interesting results in the case of two material capacitors. Significant tension loss differences between the two materials occurs, with the stiffer material, aluminum, displaying circumferential compression throughout most of the capacitor. Qualitative verification of these ply stability threatening compressive values has been obtained by unrolling several finished capacitors and finding that the interior, aluminum conducting plies were extensively and uniformly wrinkled.

There is much left to do in this area of heterogeneous wound roll analysis. Efforts to quantitatively verify predictions through controlled winding experiments is underway. Computational methods of analysis are also being pursued to open the door to more complex material models, asymmetric geometries, and asymmetric loads (7). Gross behavior of these relatively complex rolls, however, has been captured in the present analysis, and partial verification has been achieved through benchmarking against early computational approaches (7).

## REFERENCES

1. Brown, C.B. and Goodman, L.E., "Gravitational Stresses in Accreted Bodies," Proceedings of the Royal Society of London, Series A, Vol. 276, 1963, pp. 571-576.
2. Altmann, H.C., "Formulas for Computing the Stresses in Center-Wound Rolls." The Journal of the Technical Association of the Pulp and Paper Industry, Vol. 51, No. 4, 1968, pp. 176-179.
3. Yogoda, H.P., "Resolution of a Core Problem in Wound Rolls", ASME Journal of Applied Mechanics, Vol. 47, 1980, pp. 847-854.
4. Rasty, J. and Sabbaghian, M., "Effect of Imperfect Contact Between Adjacent Layers on the Integrity of Wrapped Vessels", ASME Journal of Pressure Vessel Technology, Vol. 110, 1988, pp. 247-254.
5. Reuter, R.C., Jr. and Allen, J.J., "Prediction of Mechanical States in Wound Capacitors", ASME Journal of Mechanical Design, accepted for publication.
6. Allen, J.J. and Reuter, R.C., Jr., "Optimization of Mechanical States in Wound Capacitors", ASME Journal of Mechanical Design, accepted for publication.
7. Reuter, R.C., Jr., "Mechanical and Thermochemical Stress States in Wound, Composite Rolls", Proceedings of the Fifth Japan-U.S. Conference on Composite Materials, Tokyo, Japan, June 24-27, 1990.
8. Thoinas, R.K., "Mechanical States in Wound Heterogeneous Tapes by the Finite Element Method", Proceedings of the First International Conference on Web Handling, Web Handling Research Center, Oklahoma State University, Stillwater, Oklahoma, May 19-22, 1991.